The 6th IASPEI / IAEE International Symposium: Effects of Surface Geology on Seismic Motion
August 2021

SUBSOIL NON-LINEARITY EFFECT DURING THE 2016 Mw 6.5 CENTRAL ITALY MAINSHOCK?

Di Giulio Giuseppe[1], Di Persio Manuele[1], Riccio Gaetano[1], Vassallo Maurizio[1], Cara Fabrizio[1], Cogliano Rocco[1], Cultrera Giovanna[1], Milana Giuliano[1]
1 Istituto Nazionale di Geofisica e Vulcanologia, Rome, Italy (giuseppe.digiulio@ingv.it; manuele.dipersio@ingv.it; gaetano.riccio@ingv.it; maurizio.vassallo@ingv.it; fabrizio.cara@ingv.it; rocco.cogliano@ingv.it; giovanna.cultrera@ingv.it; giuliano.milana@ingv.it)

ABSTRACT

This paper focuses on the high-frequency pulses observed in some recordings of temporary seismic stations during the largest mainshock (Mw 6.5, 30 October 2016) of the 2016-2017 Central Italy sequence. Such pulses are characterized by a spike shape and are particularly evident in the horizontal components producing peak acceleration values (PGA) that largely exceed the estimation of ground-motion prediction equation usually adopted in Italy. Similar spikes were already observed in literature for very strong earthquakes in the world, and were ascribed mostly to subsoil nonlinearity. In this work we present the raw recordings affected by the spikes of the Mw 6.5 Central Italy event, and we try to interpret these anomalous signals also invoking possible equipment malfunctions.

Keywords: soil non-linearity, site effect, 2016 Central Italy sequence

INTRODUCTION

A temporary seismic network, called 3A (doi: 10.13127/SD/ku7Xm12Yy9), was installed and operated in the epicentral area of the seismic sequence started in Central Italy on August 24th, 2016, with the Mw 6.0 Amatrice mainshock and followed by the Mw 6.5 Norcia earthquake on October 30th (Fig. 1). The network 3A consisted of 50 stations (Cara et al., 2019), installed by several Italian institutions: Istituto Nazionale di Geofisica e Vulcanologia (INGV), Consiglio Nazionale delle Ricerche (CNR) and Agenzia nazionale per le nuove tecnologie, l'energia e lo sviluppo economico sostenibile (ENEA). The network 3A produced a huge amount of records in a wide range of magnitudes (Fig. 1) and was mostly dedicated to site effects and microzonation studies (Milana et al., 2020; Priolo et al., 2020; Felicetta et al. 2021). Although the dismantling operation of the network started during the end of October 2016, some stations recorded the Mw 6.5 mainshock of 30th of October. These records provide a rare opportunity to analyze digital seismograms of one of the most energetic events occurred in the last decades in Italy (Chiaraluce et al. 2017; Scognamiglio et al. 2018), also investigating possible effects of soil nonlinearity on the ground motion. In this work we present the raw seismic data (i.e. no band-pass filtered data) of the Mw 6.5 event recorded by stations of the network 3A. We observe that the temporal traces of some stations are clearly affected by high-frequency spikes (Fig. 2). This behaviour is particularly evident in the horizontal components and gives peak values of ground acceleration (PGA) that largely exceed the estimation of the ground motion prediction equation adopted in Italy. Because several papers in literature observed a similar phenomenon during strong earthquakes and assumed that subsoil non-linearity can be one of the causes, we try to investigate whether equipment and/or deployment concerns can also explain the observed spikes.

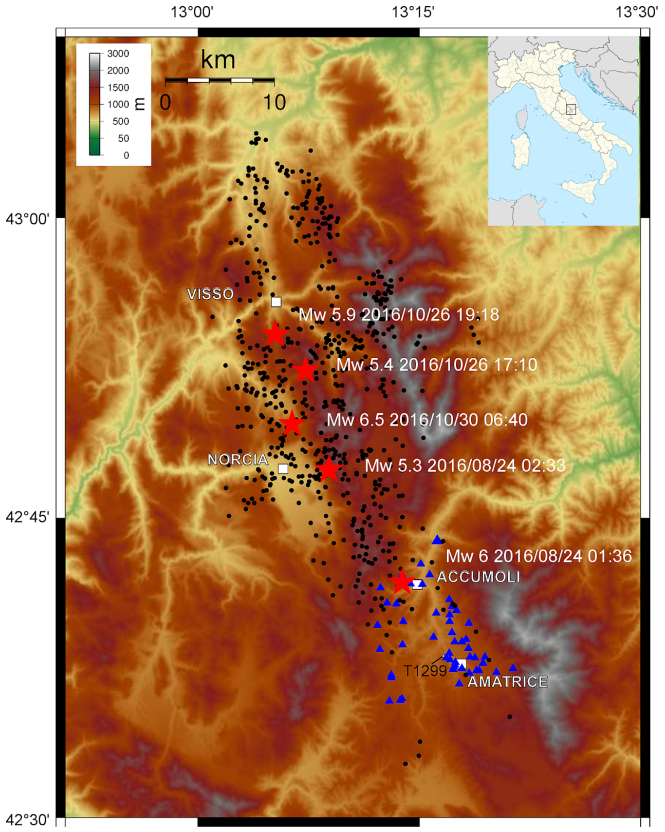

Figure 1. Stations of the network 3A are shown as blue triangles. The black dots show the events of the central Italy sequence (from a bulletin file extracted from 2016-09-19 to 2016-11-19 with magnitude > 3 and radius of 55 km from the Amatrice village). The red stars indicate the localization of the events with magnitude > 5.

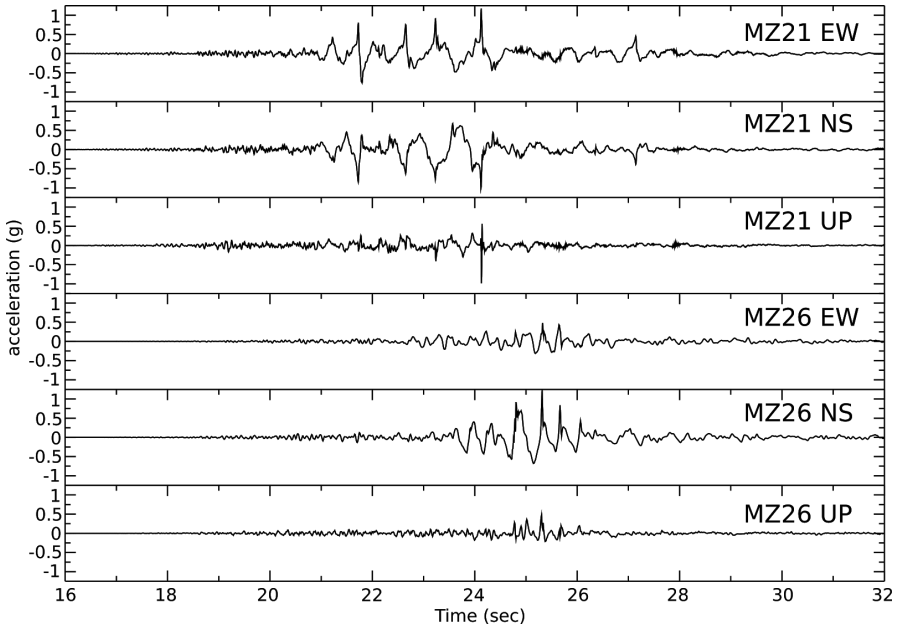

Figure 2. Mw 6.5 mainshock recorded at two sites of the network 3A (MZ21 and MZ26). From top to bottom: EW NS and UP components are shown at the two sites. Amplitude scales are acceleration in g.

DATA

The stations of the network 3A were settled in the Apennine area of Central Italy in correspondence of the Amatrice basin, where the Laga Formation (marly Flysch sandstone) represents the geological bedrock largely outcropping in the area. Depending on the predominance of its pelitic or lithoid phase, the Laga formation shows a large variability of the surface average shear-wave velocity (Vs), ranging from about 600 to 1500 m/s. Gravels and sands represent the Quaternary continental units in the basin, sometimes settled in alluvial fan and terraces (maximum sedimentary thickness of the order of 100 m). Following the EC8 seismic code (CEN 2004) and using the averaged shear-wave velocity in the uppermost 30 m (V_{S30}), most of the sites where the stations were deployed falls in the soil class B, i.e. stiff soils or weak rocks, with 360 m/s $\leq V_{S30} <$ 800 m/s. The resonance frequencies in the area vary from 1 to 10 Hz, but the majority of stations show a fundamental resonance (f_0) in the range 2-5 Hz. Details on the geological features and site characterization of the area, and results of the seismological analyses (H/V spectral ratios on noise and earthquake recordings, SSR spectral ratios using a reference station, amplification factors in different frequency bands, a site aggregation study through a cluster analysis) can be found in a recent paper by Felicetta et al. (2021). Fig. 3 shows as example the distribution of the PGA values (EW component) as functions of distance for the network 3A, pointing out that the outliers from the main trend are within the distance range 25-35 km (depending by the station position) and related to the Mw 6.5 mainshock. The PGA outliers have values from 0.1 to up nearly 1.3 g. In this work we focus in particular on the 3A stations MZ21, MZ24, MZ26, MZ28, MZ12, MZ29 and MZ08 which recorded large PGA values.

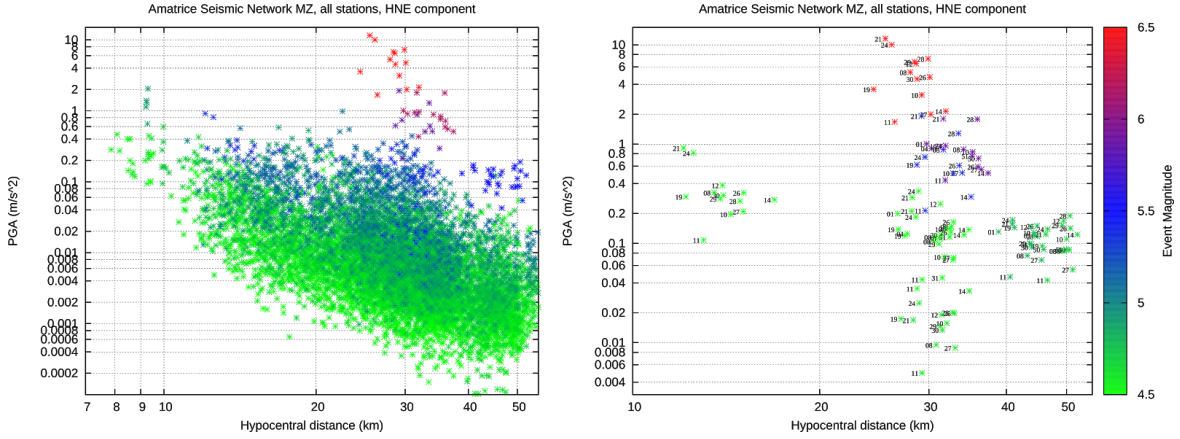

Figure 3. The left-hand column shows, for the whole network 3A, the PGA distribution of the EW component as a function of the hypocentral distance for events exceeding magnitude 3. The color scale is proportional to the magnitude. On the right-hand column, the PGA values for events with magnitude larger than 4.5 are shown (the number code indicates the stations).

The seismic stations of the network 3A recorded in continuous mode and consisted mostly of two types of 24-bit resolution digitizers: Reftek 130-01 and Quanterra Q330, coupled to force-balanced Kinemetrics Episensor EST accelerometer. Many stations were also equipped with three-components Lennartz velocimeters with eigen-frequency of 0.2 Hz (Cara et al., 2019). In this paper we used only partially the velocimeter data because of the signal saturation during the strongest event of the sequence. The gain of the digitizer was set equal to 1 and the sampling rate was fixed equal to 200 and 100 Hz for the accelerometer and velocimeter stream, respectively. The values of the input peak-to-peak full scale of the digitizers of the network are 20 V and 40 V for Reftek 130-01 and Quanterra Q330, respectively. The output full scale (one sided) of the accelerometer is 20 V for the stations considered in this paper (Table 1), with the PGA limit given by the internal jumper settings of the Episensor. The saturation level depends on the coupling between the input/output voltages of digitizer and accelerometer: for example in case of MZ08, MZ12 and MZ29 the accelerometers have a full-scale of 1g but the saturation is at 0.5 g, that is the value for which the maximum input voltage of the digitizer (10 V in absolute value) is reached (Table 1); for MZ24, MZ26 and MZ28 the

accelerometers have a full-scale of 2g and the saturation at 1g is still driven by the dynamic of the digitizer; in case of MZ21 with Q330 datalogger the saturation is at 1 g and the input range of the digitizer is fully exploited by the Episensor. The high-frequency spikes (Fig.s 4a and 4b) were observed at stations that mounted both types of digitizer (Table 1), and a clear saturation effect is evident only on the EW component of the MZ12 station (Fig. 4a) even if a clipped saturated signal is present in minor extension also at other stations (e.g. MZ24 at about 24 and 22 sec on EW and NS components, respectively). The MZ28 station, which was theoretically far from saturation (see Table 1), shows also the presence of high-frequency peaks. Further, at some stations (as MZ21) the first occurrence in the time series of the high-frequency peak seems to happen before the moment when the saturation level is reached. The same records in Fig.s 4a and 4b of the main event were plotted as a function of distance (Fig. 5), searching for an alignment of the spikes along propagation time. Indeed the presence of traveling phases in the time-space domain could suggest a source or propagation effect. Although some spikes may doubtfully appear aligned in the records (in case with a propagation of the order of around 1 sec to cover 4-5 km), it is difficult to see an overall alignment among traces.
The stations of the network 3A were deployed in free-field conditions, totally burying the accelerometer into the ground, about 20-30 cm deep (Fig. 6). The power was supplied by batteries and solar panels. The Reftek digitizer and the battery were put in an electronic plastic box (dimension 50x40x23 cm) placed a few meters far from the accelerometer. The Q330 digitizer was protected in a similar way using for each station the factory case box.

Table 1. List of the stations of the network 3A where we observed spikes during the M 6.5 event of Central Italy (occurred the 30th of October 2016).

station name	type of digitizer (full-scale)	accelerometer (Episensor with full scale)	expected saturation threshold (g)	maximum peak acceleration (absolute value on horizontal components)
MZ08	Reftek (+/-10 V)	+/-20 V (+/-1g)	+/-0.5g	0.54g
MZ12	Reftek (+/-10 V)	+/-20 V (+/-1g)	+/-0.5g	0.66g
MZ21	Q330 (+/-20 V)	+/-20 V (+/-1g)	+/-1g	1.17g
MZ24	Reftek (+/-10 V)	+/-20 V (+/-2g)	+/-1 g	1.02g
MZ26	Reftek (+/-10 V)	+/-20 V (+/-2g)	+/-1 g	1.26g
MZ28	Reftek (+/-10 V)	+/-20 V (+/-2g)	+/-1g	0.82g
MZ29	Reftek (+/-10 V)	+/-20 V (+/-1g)	+/-0.5g	0.68g

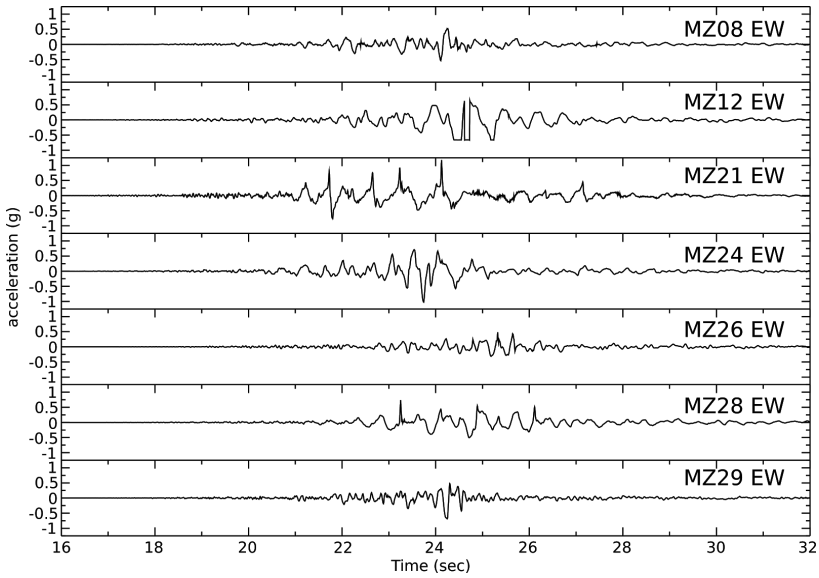

Figure 4a. EW component. Acceleration time-series of the M 6.5 mainshock for stations of Table 1.

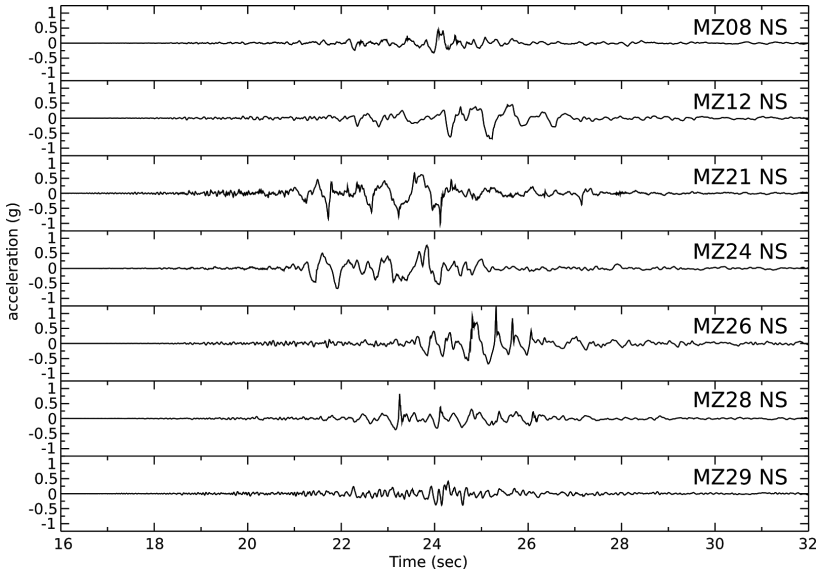

Figure 4b. NS component. Acceleration time-series of the M 6.5 mainshock for stations of Table 1.

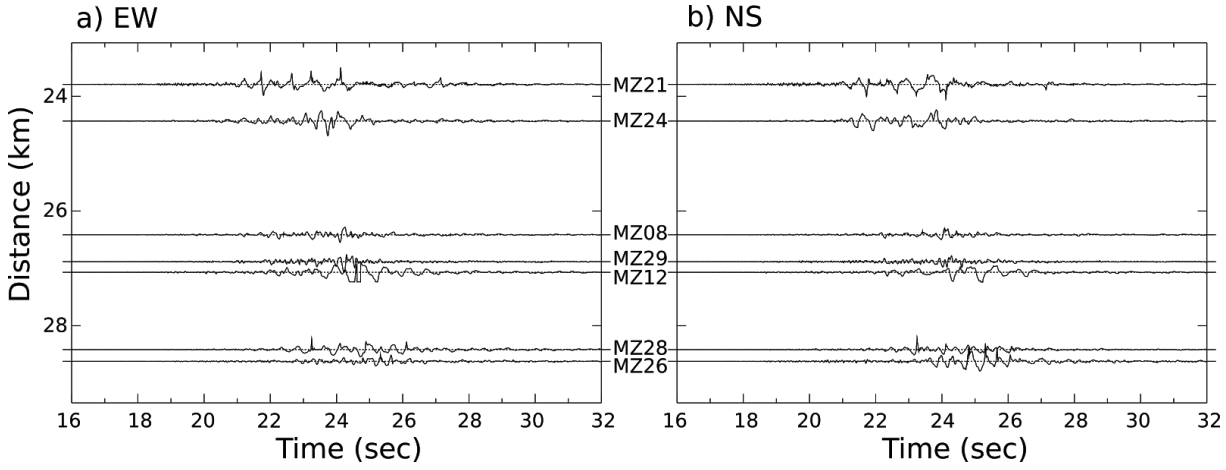

Figure 5. Record sections for the EW (panel a) and NS component (b) of the M 6.5 mainshock for the stations of Table 1 plotted as a function of the epicentral distance. Traces are normalized in amplitude.

Figure 6. Pictures showing the installation phases of MZ08 (a), MZ12 (b) and MZ21 (c). The Lennartz velocimeter and Episensor accelerometer were put inside the blue bags before being buried into the ground.

LABORATORY TEST

The observed spikes can be explained in different ways, the first being the malfunctioning of the accelerometers that were stressed over (or close to) their full scale value during the mainshock.
To investigate possible variations of functionality of accelerometers caused by the M 6.5 event, we cross-checked the weak-motion recordings for several stations following the 30th of October, taking advantage of the simultaneous presence of the velocimeter and the accelerometer. Figure 7 shows an example at station MZ21 of a small-magnitude event (M 4; 1th November 2016) occurred two days after the mainshock; the recordings of this event show a good agreement between the derivative of the velocimeter and the accelerometer data. Similar checks allow us to exclude that the Mw 6.5 event induced a permanent malfunctioning of the accelerometer. In this way, if the spikes are related to an anomalous behavior of the accelerometer, it only occurred at the largest amplitude level during the mainshock. This statement is also supported by the acceptable fit between the signals recorded by the velocimeter and accelerometer during the P- and coda- phases of the M 6.5 event (Fig. 8).

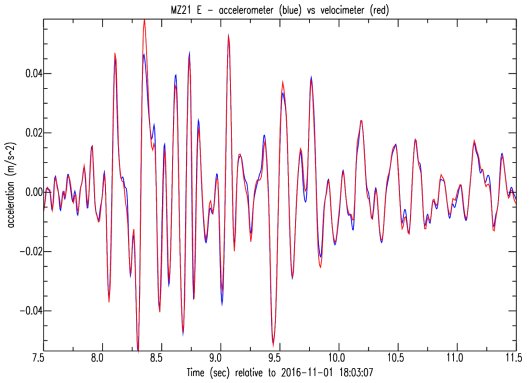

Figure 7. Comparison of the M 4 event (2016-11-01 18:03) recorded simultaneously by the velocimeter and accelerometer at the MZ21 station (EW component).

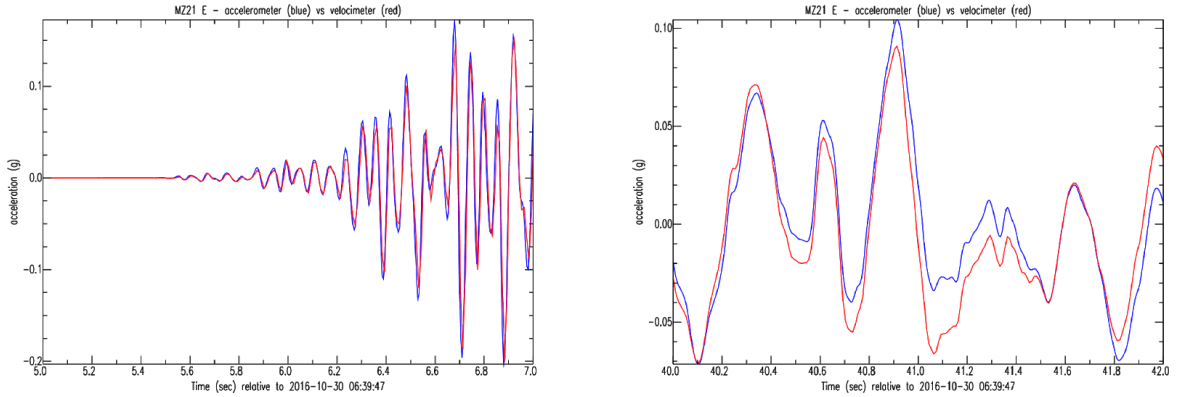

Figure 8. Comparison of the M 6.5 event recorded simultaneously by the velocimeter (red curve) and accelerometer (blue curve) at the MZ21 station (EW component). A 2 sec portion of P- and coda- phases is shown on the left and right panel, respectively. The velocimeter data are saturated for a large part of the seismic trace.

Once the stations were removed at the end of the monitoring campaign, we checked in our laboratory three Episensors showing the suspect spikes, and we did not find oxidation in the electronic parts or anomalies in comparison to the technical specifications. In particular, we built a simple circuit to test a station composed of a Reftek-130 digitizer connected to the Episensor. We first checked the Reftek digitizer alone, then the Episensor, and finally the digitizer connected to the Episensor. The digitizer input was connected to a sine-wave and a square-wave generator, and the functioning of the Episensor was tested by means of its internal calibration coil. Figure 9 shows the block diagram used for the tests and the diagram of the electronic circuit built in the laboratory. The U2 operational amplifier was configured as an analogic derivator. In Va input we have a square wave given by the square wave generator, and in U2 output we get voltage peaks at the transitions. The R8 potentiometer allows to vary as desired the amplitude of the voltage peaks. We set the sine wave and square wave frequencies to 1 Hz; the duty-cycle of the square wave was set at 50%. The capacitor C1 was chosen to have τ=R1*C1 smaller than the signal period. In this way we can highlight more the impulsive aspect of the generated signal. The operational amplifier U1 is a simple non-inverting analog adder which combines the sinusoidal wave, at the input Vb, and the voltage peaks wave. This simple circuit was assembled on a matrix board (Fig. 10). Project and realization took about an hour. The test circuit was designed to reproduce similar spikes to the ones observed in the records of the Mw 6.5 event. The input signal was sent to the Episensor and recorded as output by the Reftek (Fig.s 10 and 11), and we were able to faithfully record the input signals. The input signals were sinusoidal shapes combined to spike signals (Fig. 11) with amplitudes at different levels also approaching the saturation limit of the equipment. Figure 12 shows some other examples of signals used during the laboratory test. Additional experiment performed in the laboratory was to bury the Episensor in a basket filled with sawdust, shooting the basket by small horizontal kicks (Fig. 12c). We also manually moved the Episensor on a table to reach the saturation level of the acceleration (Fig. 13). The tests conducted in the laboratory did not show any anomalies of the instrumentation or deviation from the technical specifications of the manufactured firms.

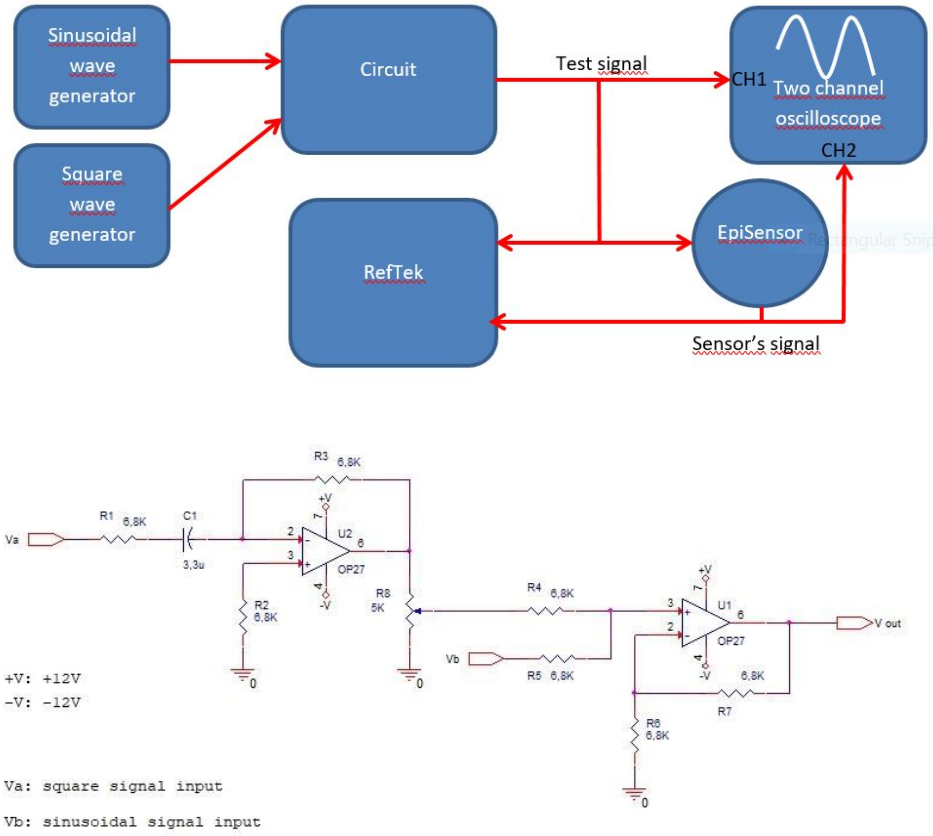

Figure 9. Block diagram and scheme of the testing circuit built in the lab.

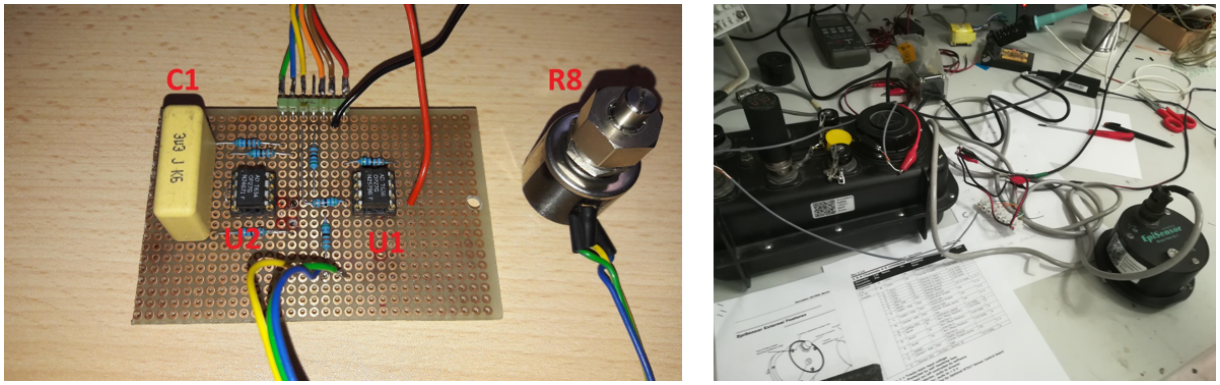

Figure 10. Left) Circuit to test the seismic instruments. Right) A phase of the Laboratory test; we sent an input signal to the Episensor, that was recorded as output by the Reftek digitizer.

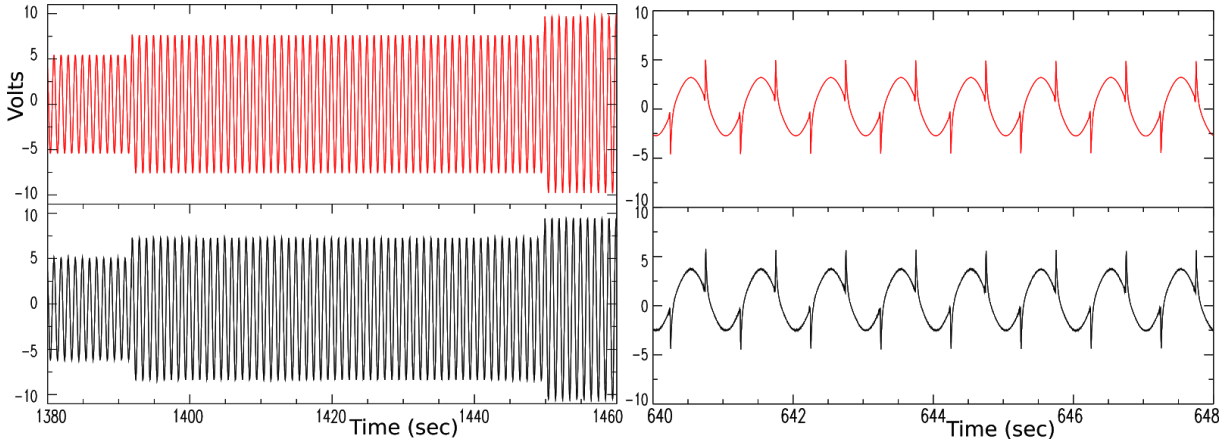

Figure 11. Input (red) and output (black) of some signals generated during the laboratory test.

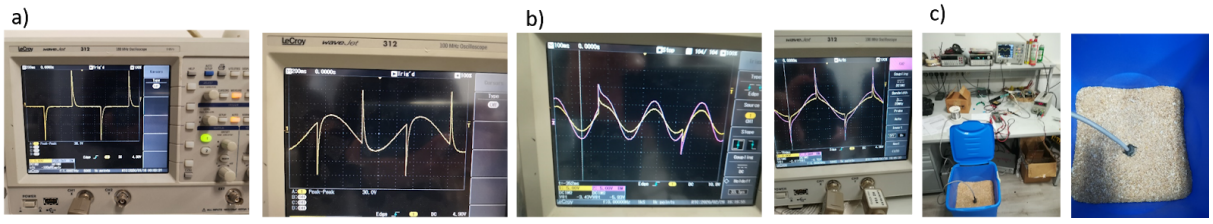

Figure 12. Signals sent during the laboratory test to the seismic station (Reftek plus Episensor). Panel a) shows an example of the input signals, panel b) compares the input signal (in yellow) to the one recorded by the digitizer (in purple; see also Fig. 11); panel c) shows the box full of sawdust with the buried Episensor.

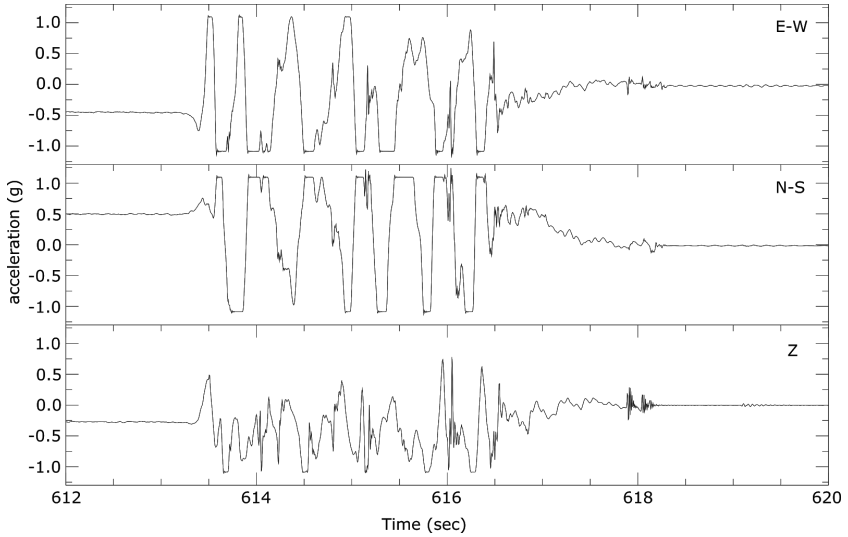

Figure 13. Test performed using a Q330 digitizer connected to the Episensor installed at station MZ21. The Episensor was manually moved in order to reach its saturation limit (at 1g). The amplitude scale is g, the x-axis is relative time (sec).

Discussion and Conclusions

During the strongest event (M 6.5) of the Central Italy 2016-2017 seismic sequence, some stations of the 3A temporary seismic network recorded high-frequency spikes which gave large values in the peak

acceleration. The observed values of peak acceleration are larger than the expected saturation level (Table 1), probably due to the fact that the effective dynamic range of the digitizers is slightly larger than the nominal one. A deviation from the zero position of the Episensor masses could also explain saturation values higher than those expected, although the Episensors tested in laboratory showed a resting mass position approaching to zero (this was true also in the testing performed before the field installation of the network 3A). The high-frequency spikes were also observed for station MZ28 (see Table 1) which recorded peak values far from the saturation level, and at many stations the spikes started before the occurrence of the clipped level. From our laboratory test, we did not evidence a malfunctioning of the instrumentations used in the field, therefore our feeling is that the origin of the anomalous high-frequency peaks cannot be related to any unexpected behaviour of the seismic instrumentation.

In principle, the high-frequency peaks observed at many stations of the network 3A could be related to some non-linear effect of the subsoil (i.e. nonlinearity). Similar spikes were already observed in seismic data of very strong earthquakes around the world, for example during the 2000 M 7.3 Tottori earthquake or the 2011 M 9.1 Tohoku earthquake (Bonilla et al. 2011; Roten et al. 2013). Observations of horizontal acceleration spikes exist also for magnitude below 7: the 2008 Mw 6.9 Iwate-Miyagi earthquake in Japan (Yamada et al. 2009; Tobita et al. 2010), the 2011 Mw 6.2 Christchurch earthquake (Fry et al 2011), or at the Wildlife site during the 1987 Ms 6.6 Imperial Valley earthquake (Holzer and Youd 2007; Zeghal and Elgamal 1994). High-frequency acceleration spikes are usually interpreted in scientific literature in connection to: i) a rapid increase in pore water pressure in subsoils susceptible to liquefaction; ii) a trampoline-like effect within loose soils with upward acceleration larger than negative ones, which is also able to explain the asymmetry usually observed in the vertical records (Aoi et al. 2008), and/or iii) to a rocking motion and subsequent collision of the observation house with the surrounding soil (Kamagata and Takewaki 2017). Forward directivity effects can also produce high-frequency pulses in near-source regions (Somerville 2003; Baker 2007) but their shapes, as reported in literature, look different from the multiple-spikes present in our recordings investigated in this work. Overall, these explanations are not truly convincing for the case of the Mw 6.5 mainshock in Central Italy. Although we do not have strong elements to exclude an effect connected to a quick increase of the pore pressure in the near-surface subsoil, significant phenomena of water leaks at the surface were not observed during the seismic sequence of Central Italy, and for this reason a link between liquefaction phenomena and spikes is difficult to sustain. Because the stations were installed almost in free-field conditions, an interaction related to the station housing has also to be excluded. To check in detail a possible influence of the typology of installation, we have compared the signals recorded at MZ08 with the ones from a co-located station (IT.AMT) belonging to the accelerometric strong-motion network managed by Italian Civil Protection Department (DPC). AMT and MZ08 were about 10 m apart from each other and both used a sampling of 200 Hz. The DPC station was composed of a Kinemetrics Basalt digitizer connected to an Episensor accelerometer. The housing of IT.AMT is illustrated in Figure 14, with the presence of a concrete basement where the accelerometer was anchored. The installation of MZ08 is also shown in Figure 6a. Data of IT.AMT were downloaded from the ESM strong-motion engineering database (Luzi et al. 2020). Figure 15 shows the accelerometric data of the M 6.5 event for the two co-located stations. The presence of high-frequency peaks occurs at MZ08 (between 13 and 15 sec in Fig. 15) and interestingly not at IT.AMT. The spikes on MZ08 appear even if the station is far from the saturation level at 0.5 g (Table 1). Also applying a low-pass filter at 40 Hz as usually done in the available strong-motion database, the high-frequency spikes of MZ08 are still present in its time series. The comparison shown in figure 15 suggests that the type of installation of the 3A stations may be the cause of the presence of the spikes. Some spikes were also produced in the laboratory by a strong shaking of the episensor (Fig. 13). A possible explanation is that the spikes during the mainshock are caused by the sensor hopping due to the severe ground motion; the accelerometers of the network 3A were just buried into the ground and not firmly anchored as the accelerometer of IT.AMT. Although additional tests and observations are necessary to understand the origin of the high-frequency spikes, the present work poses a warning to the reliability of similar spikes that can be observed in the time-series during large-magnitude events. These spikes can provide high values of peak accelerations that appear as outliers in the PGA pattern. If the interpretation of such spikes in terms of artifact is correct, these anomalous values of ground acceleration should be discarded.

Figure 14. Pictures showing IT.AMT station. MZ08 of the network 3A was co-located with the station IT.AMT, at a distance of about 10 m from each other.

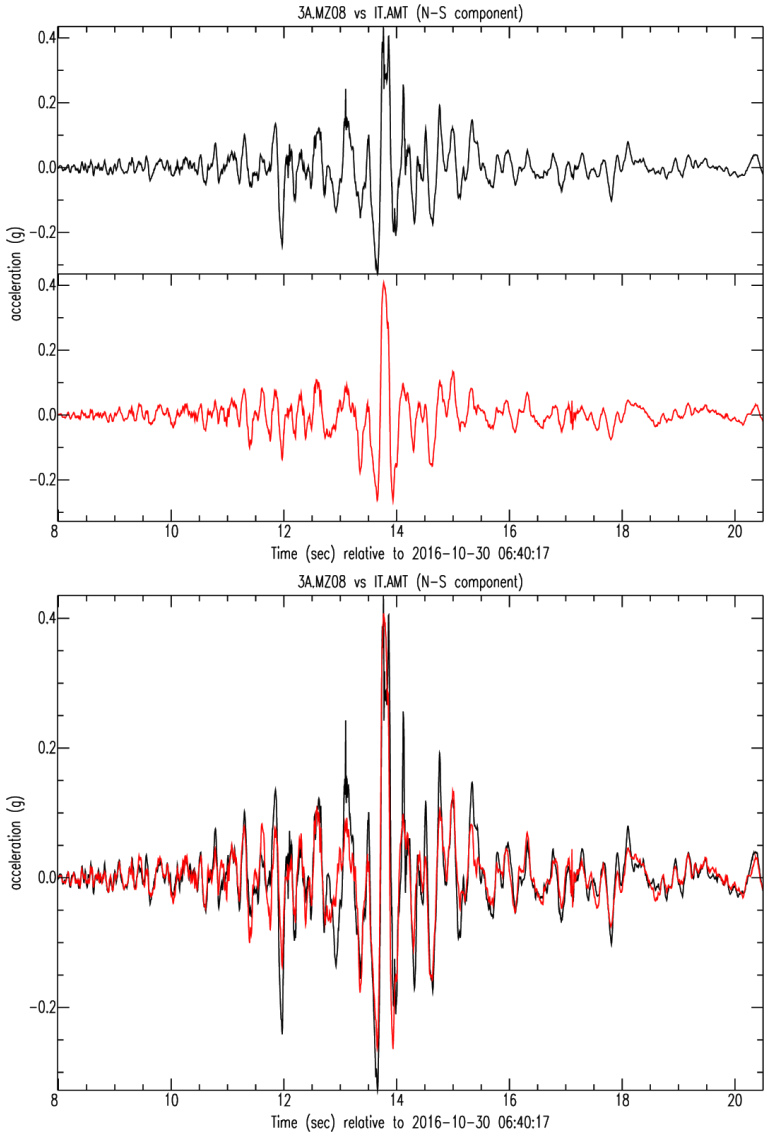

Figure 15. Recordings of the M 6.5 mainshock of Central Italy (30 October 2016) on the NS component at MZ08 and AMT stations (in black and red color, respectively). The two recordings were overlaid in the bottom panel.

REFERENCES

Aoi, S., Kunugi, T., and Fujiwara, H. (2008). "Trampoline effect in extreme ground motion", *Science,* **322**(5902), pg. 727

Baker, J.W., (2007). "Quantitative classification of near-fault ground motions using wavelet analysis", *Bull. Seism. Soc. Am.*, **97**(5), pp.1486-1501.

Bonilla L., Gelis C., Regnier J. (2011). "The challenge of nonlinear site response: field data observations and numerical simulations", *4th IASPEI/IAEE International Symposium: Effects of Surface Geology on Seismic Motion*, August 23-26, 2011, University of Santa Barbara.

Cara, F., Cultrera, G., Riccio, G. et al. (2019). "Temporary dense seismic network during the 2016 Central Italy seismic emergency for microzonation studies". *Sci Data,* **6**(182), https://doi.org/10.1038/s41597-019-0188-1.

CEN (2004). Eurocode (EC) 8: Design of structures for earthquake resistance – Part 1 General rules, seismic actions and rules for buildings (EN 1998-1), Brussels.

Chiaraluce, L., Di Stefano, R., Tinti, E., et al. (2017). "The 2016 central Italy seismic sequence: A first look at the mainshocks, aftershocks, and source models". *Seismological Research Letters*, **88**(3), pp.757-771.

Felicetta, C., Mascandola, C., Spallarossa, D., Pacor, F., Hailemikael, S. and Di Giulio, G. (2021). "Quantification of site effects in the Amatrice area (Central Italy): Insights from ground-motion recordings of the 2016–2017 seismic sequence". *Soil Dynamics and Earthquake Engineering*, **142**, https://doi.org/10.1016/j.soildyn.2020.106565.

Fry, B., Benites, R., and Kaiser, A. (2011). "The Character of accelerations in the Mw 6.2 Christchurch earthquake", *Seism. Res. Lett.*, **82**(6), pg. 846-852.

Holzer, T.L. and Youd, T.L., (2007). "Liquefaction, ground oscillation, and soil deformation at the Wildlife Array", California. *Bull. Seism. Soc. Am.*, **97**(3), pp.961-976.

Kamagata, S. and Takewaki, I., (2017). "Occurrence Mechanism of large acceleration in KiK-net seismic records during iwate–Miyagi nairiku earthquake in 2008". *Frontiers in Built Environment*, **3**, p.13.

Luzi L., Lanzano G., Felicetta C., D'Amico M. C., Russo E., Sgobba S., Pacor, F., & ORFEUS Working Group 5 (2020). "Engineering Strong Motion Database (ESM) (Version 2.0)". *Istituto Nazionale di Geofisica e Vulcanologia (INGV)*. https://doi.org/10.13127/ESM.2

Milana, G., Cultrera, G., Bordoni, P. et al. (2020). "Local site effects estimation at Amatrice (Central Italy) through seismological methods". *Bull Earthquake Eng*, **18**, 5713–5739, https://doi.org/10.1007/s10518-019-00587-3

Priolo, E., Pacor, F., Spallarossa, D. et al. (2020). "Seismological analyses of the seismic microzonation of 138 municipalities damaged by the 2016–2017 seismic sequence in Central Italy", *Bull Earthquake Eng*, **18**, 5553–5593, https://doi.org/10.1007/s10518-019-00652-x

Roten, D., Fäh, D. and Bonilla, L.F., (2013). "High-frequency ground motion amplification during the 2011 Tohoku earthquake explained by soil dilatancy". *Geophysical Journal International,* **193**(2), pp.898-904.

Scognamiglio, L., Tinti, E., Casarotti, E., Pucci, S., Villani, F., Cocco, M., Magnoni, F., Michelini, A. and Dreger, D., (2018). "Complex fault geometry and rupture dynamics of the MW 6.5, 30 October 2016, Central Italy earthquake", *Journal of Geophysical Research: Solid Earth*, **123**(4), pp.2943-2964.

Somerville, P. G. (2003). "Magnitude scaling of the near fault rupture directivity pulse", *Phys. Earth Planet. Interiors,* **137**(1), 12.

Tobita, T., Iai, S., and Iwata, T. (2010). "Numerical analysis of near-field asymmetric vertical motion". *Bull. Seism. Soc. Am.* **100**, 1456-1469.

Yamada, M., Mori, J. and Heaton, T., (2009). "The slapdown phase in high-acceleration records of large earthquakes". *Seismological Research Letters*, **80**(4), pp.559-564.

Zeghal, M. and Elgamal, A.W., (1994). "Analysis of site liquefaction using earthquake records". *Journal of geotechnical engineering*, **120**(6), pp.996-1017.